Electronic Supplementary Information (ESI)

3D Printed Microfluidic Circuitry *via* Multijet-Based Additive Manufacturing

R. D. Sochol,‡[abcd]   E. Sweet,[ab]   C. C. Glick,[be]   S. Venkatesh,[ab]   A. Avetisyan,[f]
K. F. Ekman,[ab] A. Raulinaitis,[ab] A. Tsai,[bg] A. Wienkers,[ab] K. Korner,[ab] K. Hanson,[bg]
A. Long,[bg] B. J. Hightower,[abh] G. Slatton,[ab] D. C. Burnett,[bi] T. L. Massey,[bi] K. Iwai,[ab]
L. P. Lee,[bg] K. S. J. Pister[bi] and L. Lin§[ab]

a. Department of Mechanical Engineering, University of California, Berkeley, USA
b. Berkeley Sensor and Actuator Center, USA
c. Department of Mechanical Engineering, University of Maryland, College Park, USA
d. Fischell Department of Mechanical Engineering, University of Maryland, College Park, USA
e. Department of Physics, University of California, Berkeley, USA
f. Department of Process Engineering, Swiss Federal Institute of Technology, Zurich, Switzerland
g. Department of Bioengineering, University of California, Berkeley, USA
h. Department of Mechanical Engineering, Stanford University, Stanford, CA, USA
i. Department of Electrical Engineering and Computer Sciences, University of California, Berkeley, USA

‡ Ryan D. Sochol, 2147 Glenn L. Martin Hall, Building 088, University of Maryland, College Park, MD 20742, USA; rsochol@umd.edu

§ Liwei Lin, 621E Sutardja Dai Hall, University of California, Berkeley, CA 94720, USA; lwlin@me.berkeley.edu

ESI Text
ESI Figures S1-S8
ESI Movies S1-S7

ESI Text

3D Full-Wave Fluidic Bridge Rectifier Functionality

Circuit diagrams and conceptual illustrations corresponding to the sequential fluidic routing operations of the 3D printed full-wave fluidic rectifier are shown in ESI Figure S5 (*see also* ESI Movie S4). For the State 1 case (ESI Fig. S5a), the pressure applied to the left supply port (ESI Fig. S5a – "+") is larger than the pressure applied to the right supply port (ESI Fig. S5a – "-"). The resulting pressure gradient induces fluid flow through the supply port to the left fluidic node (*i.e.*, channel-channel junction) (ESI Fig. S5a – *i*), which is connected to both the forward flow input port of the top-left fluidic diode and the reverse flow port of the bottom-left fluidic diode. Due to the 3D fluidic diode design (Fig. 1d), this arrangement obstructs the flow of fluid through the bottom-left fluidic diode, while allowing for fluid to be transported through the top-left fluidic diode, to the top fluidic node (ESI Fig. S5a – *ii*). The top fluidic node is also connected to both the top outlet port and the reverse flow input port of the top-right fluidic diode. Consequently, fluid is directed out of the top output port (through a flow sensor in series) and then back into the bottom output port (ESI Fig. S5a – *iii*, *dotted arrow*) to the bottom fluidic node (ESI Fig. S5a – *iii*). Although the bottom fluidic node is connected to the forward flow input port of the bottom-left fluidic diode, the pressure at the left fluidic node is greater than the pressure at the bottom node – a pressure gradient that hinders fluid flow through the bottom-left diode. The bottom fluidic node is also connected to the forward flow input port of the bottom-right fluidic diode, which promotes the flow of fluid through the component to the right fluidic node (ESI Fig. S5a – *iv*). Similar to the case for the bottom fluidic node, the right fluidic node is connected to the forward flow input

port of the top-right fluidic diode; however, the pressure difference between the top and right fluidic nodes prevents fluid from flowing through the component. Instead, fluid is directed out the right supply port (ESI Fig. S5a – *v*, "-").

For the State 2 case (ESI Fig. S5b), the pressure applied to the right supply port (ESI Fig. S5b – "+") is larger than the pressure applied to the left supply port (ESI Fig. S5b – "-"). In contrast to the State 1 case, this pressure gradient induces fluid flow through the right supply port to the right fluidic node (ESI Fig. S5b – *i*), which is connected to both the forward flow input port of the top-right fluidic diode and the reverse flow port of the bottom-right fluidic diode. In this case, fluid flow is promoted through the top-right fluidic diode to the top fluidic node (ESI Fig. S5b – *ii*), which is connected to the reverse flow input port of the top-left fluidic diode. Consistent with flow path for the State 1 case, fluid is transported from the top fluidic node, out of the top output port, and then back into the bottom output port (ESI Fig. S5b – *iii*, *dotted arrow*) to the bottom fluidic node (ESI Fig. S5b – *iii*). In the State 2 case, however, the pressure at the right fluidic node is greater than the pressure at the bottom node, which results in fluid flowing from the bottom fluidic node, through the forward flow input port of the bottom-left fluidic diode, to left fluidic node (ESI Fig. S5b – *iv*). Due to a similar pressure gradient across the top-left fluidic diode, fluid flow is then directed out of the left supply port (ESI Fig. S5b – *v*, "-"). Thus, despite the opposite polarities of the supply inputs (ESI Fig. S5 – "+" and "-") for the State 1 and State 2 cases, the flow polarity across the outputs (ESI Fig. S5 – *dotted arrows*) remains constant.

ESI Fig. S1 | Simultaneous fabrication of multiple 3D IFC components and systems *via* multijet modelling (MJM). (**a**) Time-lapse images of the photocurable

plastic resin and sacrificial wax support materials being 3D printed layer-by-layer to construct multiple IFC components and systems simultaneously in parallel (*see also* ESI Movie S1). (**b**-**d**) Images of the IFC devices on the aluminium build plate inside the 3D printer after completion of the fabrication processes (approximately 5.5 hours). (**e**) Image of the 3D printed devices after being removed from the aluminium substrate, but prior to the sacrificial wax development process. The demonstrative 3D print shown includes one fluidic capacitor, six fluidic diodes, ten fluidic transistors without gain enhancement, one fluidic transistor with gain enhancement, one full-wave fluidic bridge rectifier with a planar architecture, one full-wave fluidic bridge rectifier with a vertically-stacked architecture, and one multi-flow controller system. (**f**-**i**) Fabrication results for 3D printed fluidic circuit components following the wax removal process and then filled with dye-coloured fluids. (**f**) 1 cm-in-diameter (*left*) and 2 cm-in-diameter (*right*) 3D printed fluidic capacitors. (**g**) 3D printed fluidic diode. (**h**) 3D printed fluidic transistor without gain-enhancement. (**i**) 3D printed fluidic transistor with gain-enhancement.
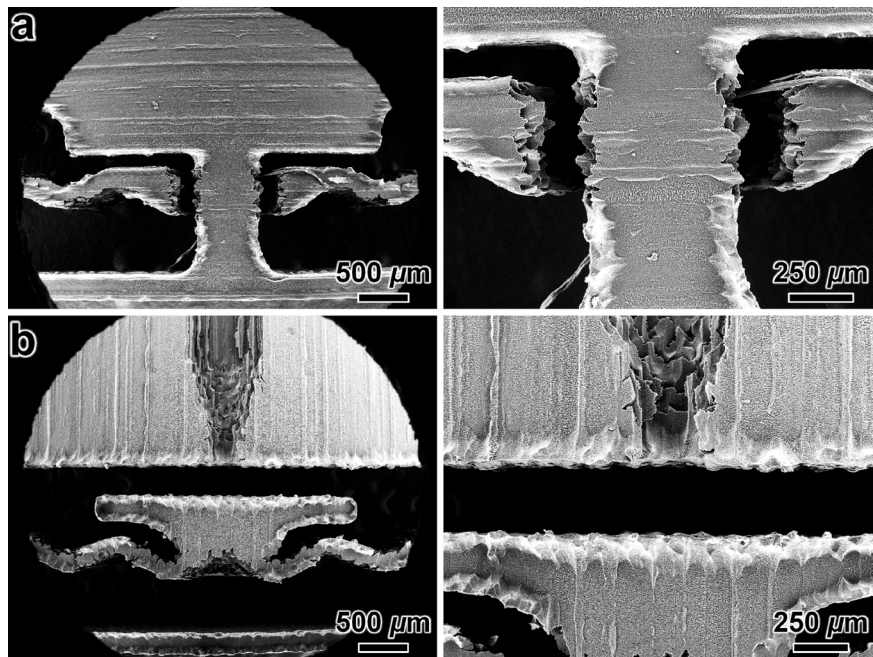
ESI Fig. S2 | 3D printing fabrication results. Scanning electron micrographs showing

the key interfaces of the 3D printed (**a**) fluidic diode, and (**b**) fluidic transistor.
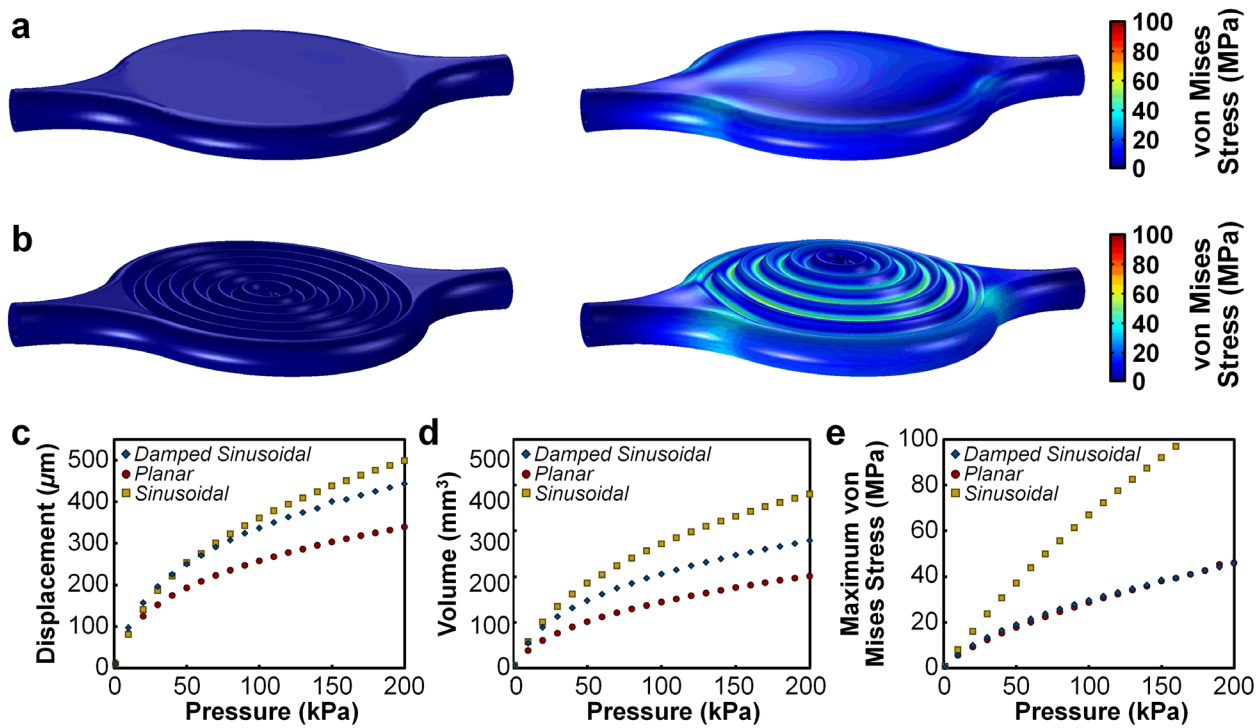
ESI Fig. S3 | Theoretical simulation results for 3D fluidic capacitor functionalities corresponding to varying diaphragm designs. (**a**, **b**) Simulation results for deformation and von Mises stress distributions under 0 kPa (*left*) and 200 kPa (*right*) for the (**a**) planar design, and (**b**) undamped sinusoidal design. (**c**-**e**) Theoretical simulation results for 3D fluidic capacitor (**c**) diaphragm displacement, (**d**) volume change, and (**e**) maximum von Mises stress *versus* varying input air pressure corresponding to different diaphragm cross-sectional designs. All simulations are for 1 cm-in-diameter 3D fluidic capacitors.
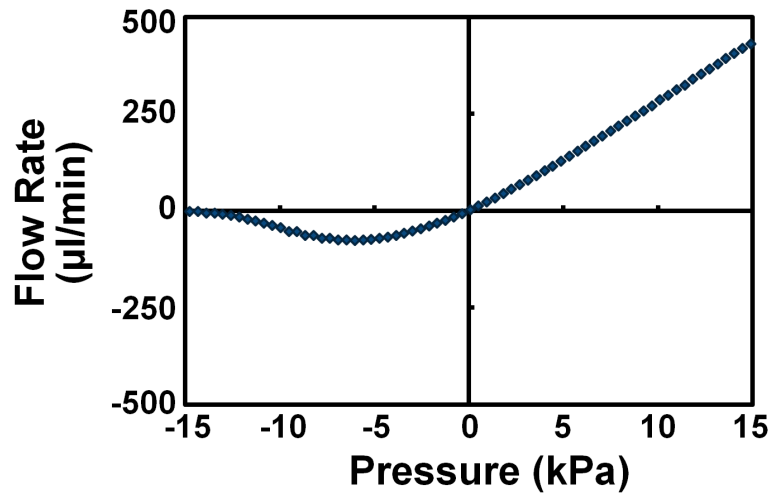
ESI Fig. S4 | Theoretical simulation results for directional fluid flow *versus* input pressure for the 3D fluidic diode. Forward pressure and flow rate values denote positive pressure/flow in the forward direction (*i.e.*, inputted *via* the top inlet ports); Negative pressure and flow rate values denote positive pressure/flow in the reverse direction (*i.e.*, inputted *via* the bottom inlet ports).
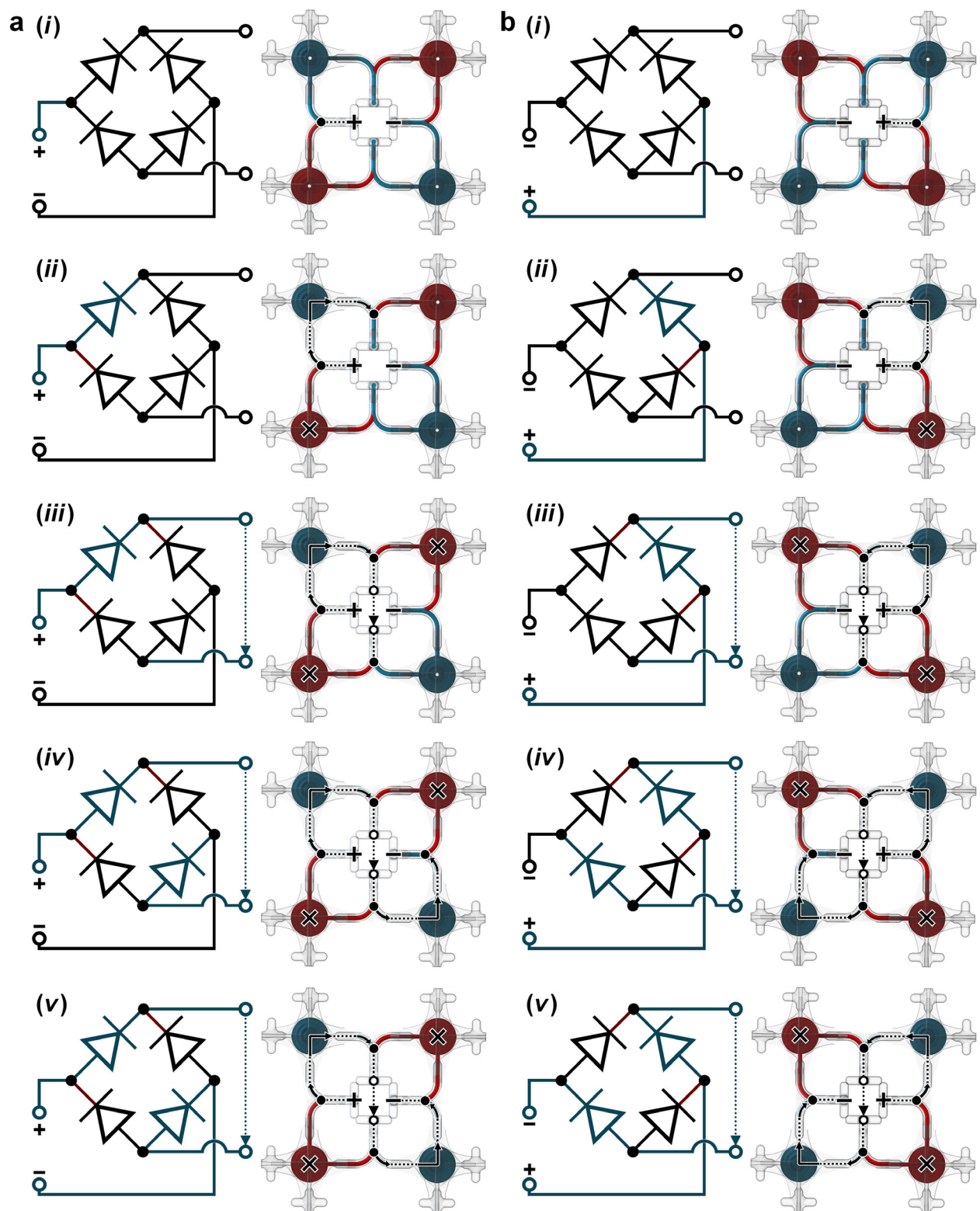
ESI Fig. S5 | 3D full-wave fluidic bridge rectifier functionality. Sequential circuit

diagrams (*left*) and conceptual schematics (*right*) of the 3D full-wave fluidic bridge

rectifier for the two primary flow states: (**a**) State 1 and (**b**) State 2 (*see also* ESI Movie S4). *Red* and *teal colours* denote obstructed and unobstructed fluid flow, respectively; *Dotted lines* and *arrows* denote primary flow paths; "X" marks denote 3D fluidic diodes in which the flow of fluid is obstructed; *Black-filled circles* denote fluidic nodes; *White-filled circles* denote output ports for the conceptual schematics.
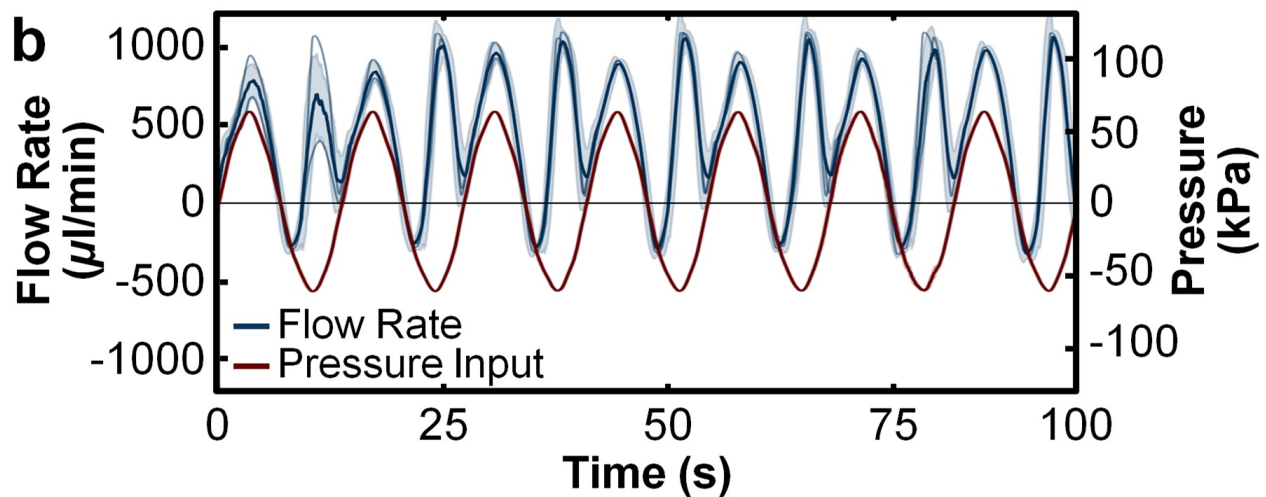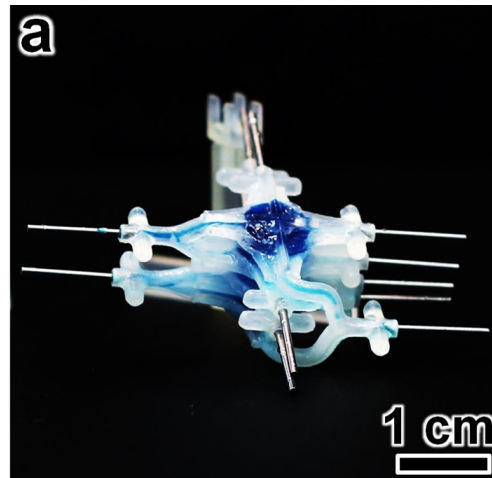
ESI Fig. S6 | 3D printed full-wave fluidic bridge rectifier with vertically-stacked architecture. (**a**) Fabrication results. (**b**) Experimental results for full-wave fluidic rectification. Error bands denote standard deviation; Negative pressures/flow rates denote positive pressure/flow in the reverse direction.

a

von Mises Stress (MPa)
0 10 20 30 40 50

Fluid Velocity
Magnitude (mm/s)
0 200 400 600 800

b

Flow Rate (µl/min) vs P_S (kPa)

P_G (kPa)
- 34
- 36
- 38
- 40
- 42
- 44
- 46
- 48
- 50
- 52

c

Flow Rate (µl/min) vs P_G (kPa)

P_S (kPa)
- 35
- 70
- 100
- 135
- 170
- 200
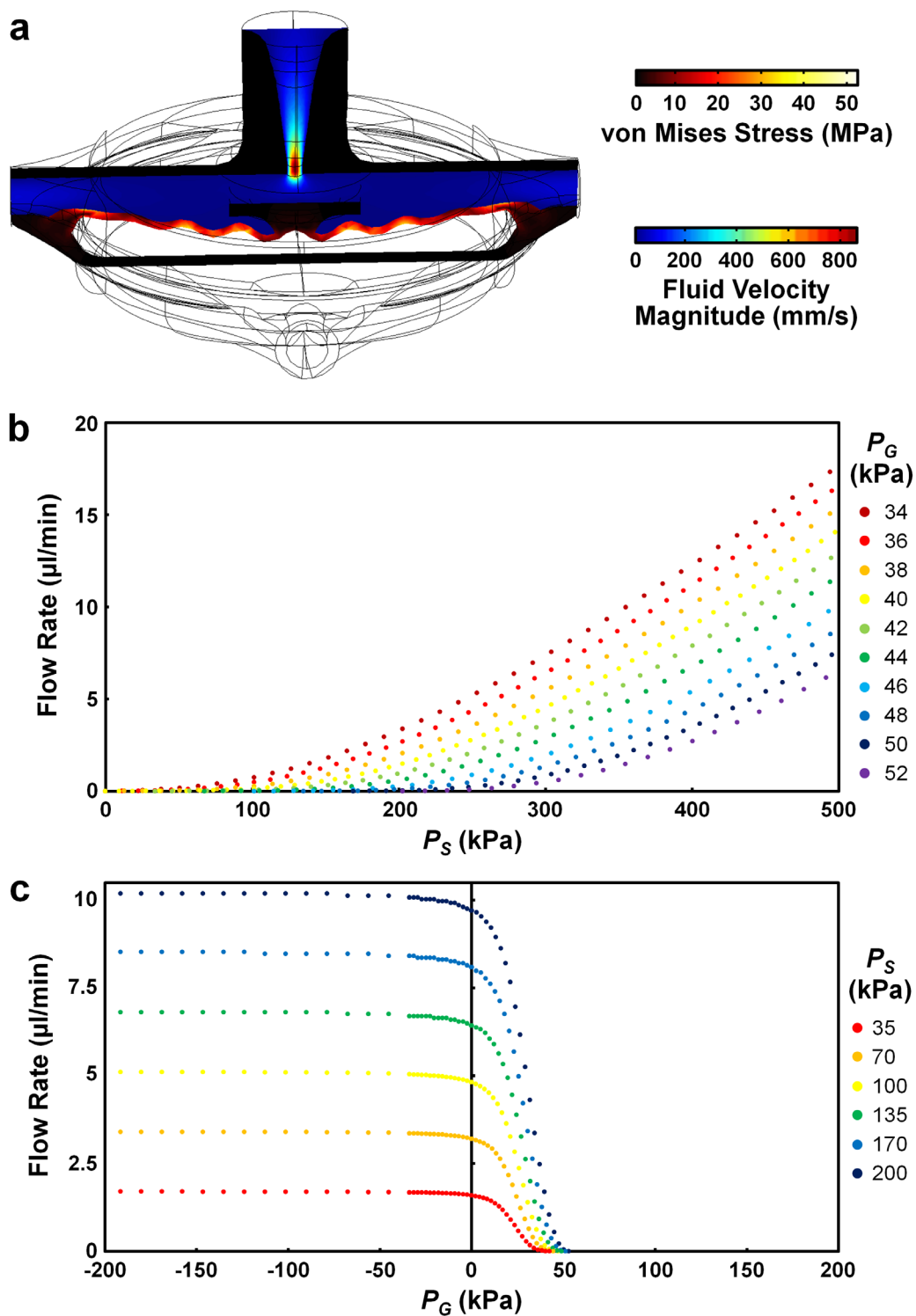
ESI Fig. S7 | Theoretical simulation results for the 3D fluidic transistor. (**a**) Cross-sectional view of theoretical simulation results for fluid velocity field and von Mises stress distributions of the 3D fluidic transistor for P_S = 30 kPa and P_G = -200 kPa

12

(vacuum; *see also* ESI Movie S4). (**b**) Simulation results for source-to-drain fluid flow (Q_{SD}) *versus* varying P_S for distinct, constant P_G inputs. (**c**) Simulation results for Q_{SD} *versus* varying P_G for distinct, constant P_S inputs.

a $f(x) = 175\,\mu m \times \sin\left(6x + \frac{\pi}{2}\right) \times \left(1 - \frac{x}{4\pi/3}\right)$

1.25 mm · 150 μm · 450 μm · 750 μm · 1.5 cm

b $f(x) = 350\,\mu m \times \sin\left(6x + \frac{\pi}{2}\right) \times \left(1 - \frac{x}{3\pi}\right)$

$D_S = 1$ cm · $D_S = 2$ cm · 2 mm · 150 μm · 800 μm · 750 μm · 3.5 cm

c $D = 1$ cm · 2 mm · 150 μm · 200 μm · 600 μm · 1.9 mm · 750 μm · 100 μm · 250 μm · 1.1 cm

d $D = 1$ cm · 750 μm · 1.25 mm · D_{PS} · 150 μm · 300 μm · 250 μm · 1.9 mm · 1.25 mm · 2.5 mm · 750 μm · 1.1 cm

e $D = 1$ cm · $D = 2$ cm · D_{PS} · 2 mm · 300 μm · 2.5 mm · 1 cm · 1.25 mm · 1 mm · 750 μm · 3.1 cm
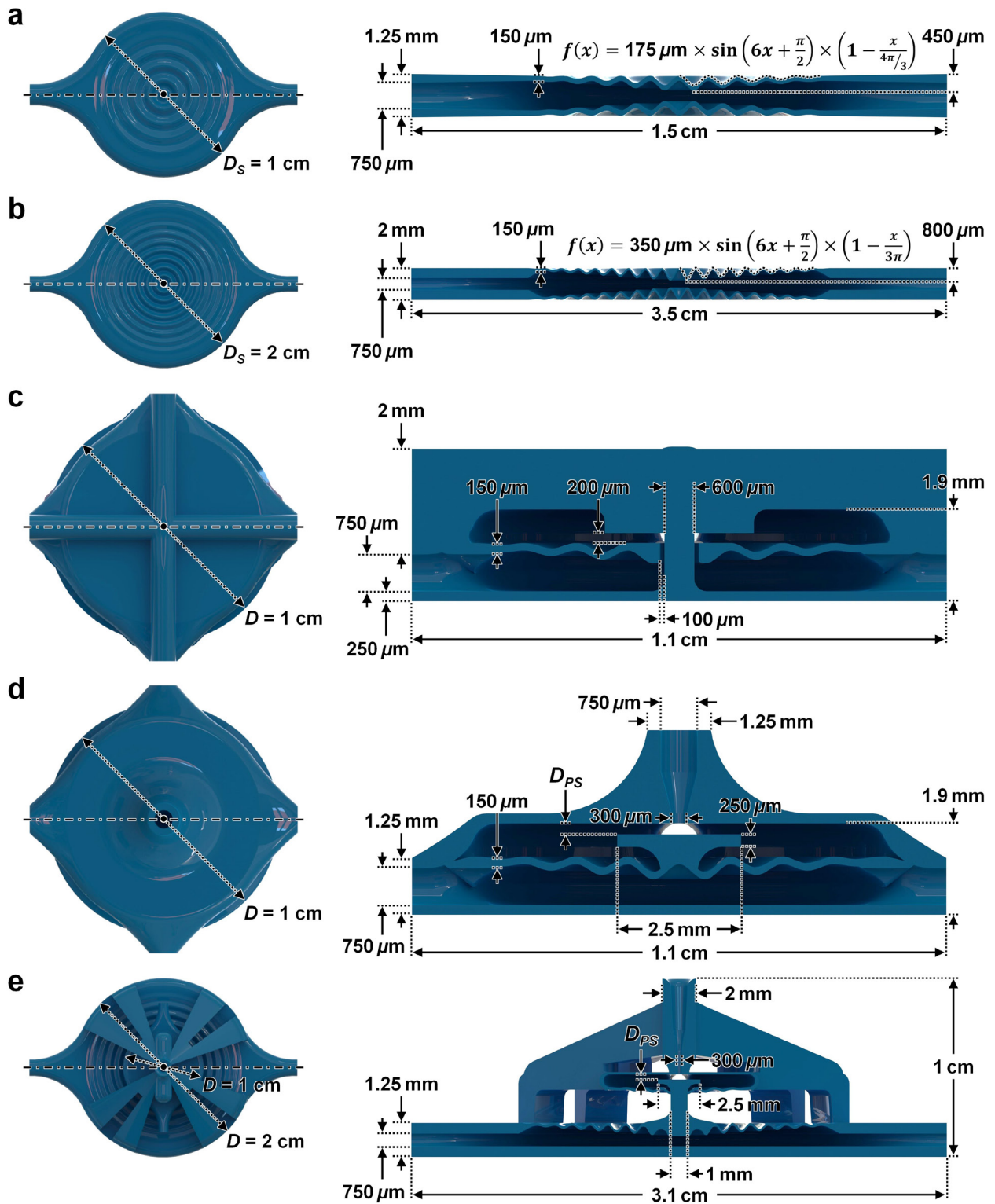
Figure S8 | Dimensioned diagrams for the 3D fluidic circuit components. (**a**) 1 cm-in-diameter 3D fluidic capacitor design. (**b**) 2 cm-in-diameter 3D fluidic

14

capacitor design. (**c**) 3D fluidic diode. (**d**) 3D fluidic transistor. (**e**) 3D fluidic transistor with gain enhancement. The damped sinusoidal designs for the diaphragm elements of the fluidic diode, fluidic transistor, and the source region of the fluidic transistor with gain enhancement are described by the equation in (**a**). The damped sinusoidal design for the diaphragm element in the gate region of the fluidic transistor with gain enhancement is described by the equation in (**b**). The distance between the top surface of the piston and the source output (D_{PS}) in (**d**, **e**) can be modulated to influence 3D fluidic component functionalities.

ESI Movie Captions

ESI Movie S1. Experimental results for the fabrication of 3D printed fluidic circuit components and systems *via* the multijet modelling (MJM) process. Video captured over the course of the 5.5 hour process of the photocurable plastic and sacrificial wax support materials being 3D printed layer-by-layer to construct multiple components and systems simultaneously and in parallel.

ESI Movie S2. Theoretical simulation results for the 3D fluidic capacitor. Deformation and von Mises stress distributions under varying input pressure for the 3D printed fluidic capacitor (1 cm-in-diameter; damped sinusoidal design).

ESI Movie S3. Theoretical simulation results for the 3D fluidic diode. Cross-sectional view of deformation, fluid velocity field, and von Mises stress distributions under varying input pressure for the 3D printed fluidic diode.

ESI Movie S4. **Theoretical simulation results for the 3D fluidic transistor.** Cross-sectional view of for deformation, fluid velocity field, and von Mises stress distributions under a constant P_S and varying P_G for the 3D printed fluidic transistor (without gain enhancement).

ESI Movie S5. Experimental results for the 3D printed P_G-actuated multi-flow controller. Proportions of discrete dye-colored fluidic streams corresponding to constant P_S = 1 kPa and varying P_G.

ESI Movie S6. CAD-based assembly process for a 3D printed fluidic circuit design. Desired 3D fluidic component models are imported into an assembly file. The

components are mated at specified locations corresponding to the component design. For this case, a circuit is assembled that includes a 3D fluidic capacitor (*blue*), diode (*red*), resistor (*white – curved*), transistor without gain-enhancement (*green*), resistor (*white – straight*), and transistor with gain-enhancement (*yellow*) connected in series. Chip-to-world interconnects in the form of ports (*black*) are included for fluidic inputs, outputs, and controls.